Upconversion Loop Oscillator Axion Detection Experiment: A Precision Frequency Interferometric Axion Dark Matter Search with a Cylindrical Microwave Cavity

Catriona A. Thomson,* Ben T. McAllister, Maxim Goryachev, Eugene N. Ivanov, and Michael E. Tobar†
ARC Centre of Excellence for Engineered Quantum Systems and ARC Centre of Excellence for Dark Matter Particle Physics, Department of Physics, University of Western Australia, 35 Stirling Highway, Crawley, Western Australia 6009, Australia

(Received 5 January 2020; revised 11 November 2020; accepted 15 January 2021; published 23 February 2021)

First experimental results from a room-temperature tabletop phase-sensitive axion haloscope experiment are presented. The technique exploits the axion-photon coupling between two photonic resonator oscillators excited in a single cavity, allowing low-mass axions to be upconverted to microwave frequencies, acting as a source of frequency modulation on the microwave carriers. This new pathway to axion detection has certain advantages over the traditional haloscope method, particularly in targeting axions below 1 μeV (240 MHz) in energy. At the heart of the dual-mode oscillator, a tunable cylindrical microwave cavity supports a pair of orthogonally polarized modes ($TM_{0,2,0}$ and $TE_{0,1,1}$), which, in general, enables simultaneous sensitivity to axions with masses corresponding to the sum and difference of the microwave frequencies. However, in the reported experiment, the configuration was such that the sum frequency sensitivity was suppressed, while the difference frequency sensitivity was enhanced. The results place axion exclusion limits between 7.44–19.38 neV, excluding a minimal coupling strength above 5×10^{-7} 1/GeV, after a measurement period of two and a half hours. We show that a state-of-the-art frequency-stabilized cryogenic implementation of this technique, ambitious but realizable, may achieve the best limits in a vast range of axion space.

DOI: 10.1103/PhysRevLett.126.081803

The nature of dark matter in our universe has long been a looming question in physics and the focus of extensive experimental efforts today. Weakly interacting sub-eV particles (WISPs) are becoming increasingly suspect in the wake of sustained nondetection by high-mass experiments [1]. The axion, a theorized Nambu-Goldstone boson emerging from the Peccei-Quinn (PQ) solution to the strong charge-parity (CP) problem in quantum chromodynamics (QCD) [2–4], is a popular candidate for cold dark matter, with a mass poorly constrained by theory; several orders of magnitude are available for exploration [5–8]. The majority of axion experiments that aim to detect the QCD axion are "haloscopes," which are sensitive to power deposition from the conversion of galactic halo axions into photons through the inverse Primakoff effect, as predicted by the axion-augmented QCD Lagrangian [9–12]. Experiments such as the well-established Axion Dark Matter eXperiment (ADMX) [13–15], the ORGAN Experiment [16], HAYSTAC [17], and CULTASK [18] have hitherto depended upon low-noise microwave receivers and cryogenic cooling to detect excess real microwave photons produced in a low-loss microwave cavity surrounded by a strong dc magnetic field.

Our approach similarly employs an electromagnetic resonance in a low-loss microwave cavity, but instead of inducing axion-photon conversion by applying an external dc magnetic field, we excite another resonance within the cavity to act as the second source of photons. The spatial overlap between the E field of one mode in the cavity with the B field of the other induces the desired coupling. We dub this configuration the ac haloscope, in reference to the dc field normally employed in haloscope experiments. The configuration was conceived from the observation that while most haloscopes attempt to scatter axions off a virtual photon source, the Primakoff process also generates products in the presence of real photons, as noted by Sikivie in 2010 [19]. An axion with an energy corresponding to the sum or difference frequency of the photons is expected to interact and may be detected via frequency [20] or power measurements [19,21,22]. Uniquely, the ac haloscope allows one to search for an axion signal imprinted in the phases of the photon modes, placing it in a new class of haloscopes, focused on frequency metrology, instead of power detection [20]. The power detection approach is not elaborated upon in this work as, inherently, frequency techniques are orders of magnitude more sensitive than power techniques (see Supplemental Material for further details [23]), and have been used in the past for some of the best tests of fundamental physics, including variations in fundamental constants and local position invariance [38–40], as well as tests of Lorentz invariance violation [41–43], with proven long-term performance of up to eight years [40], and if designed properly the sensitivity will be determined by the white frequency noise floor of the frequency stabilization system [41].

The experiment in this work comprises a resonant cavity supporting two spatially overlapping microwave modes via two free-running loop oscillators. Our chosen geometry has enhanced sensitivity to upconversion (photon difference) at the expense of downconversion (photon sum), which is detailed in the Supplemental Material. As a result, we present the UPLOAD (UPconversion Loop Oscillator Axion Detection) experiment using a cylindrical microwave cavity (UPLOAD-CMC), with the schematic shown in Fig. 1. By searching for frequency deviations of the carrier frequencies of the oscillators, this experiment can be configured to cover a large portion of unexplored low-mass axion space, below the ADMX mass range, i.e., from dc to 240 MHz (< 1 μeV).

Experimentally, this design enables a coherent phase or frequency modulation induced by the axion-photon interaction to be scanned. The large signal effective noise temperature of the sustaining loop amplifier limits the system's frequency stability and therefore our ability to sense the predicted modulation. The results produced in this experiment place limits on axion-photon coupling in the MHz range by observing the absence of axion-induced frequency modulation in orthogonally oriented photonic modes oscillating within a small cylindrical copper cavity at room temperature.

The axion-photon interaction Hamiltonian density is familiarly parameterized as

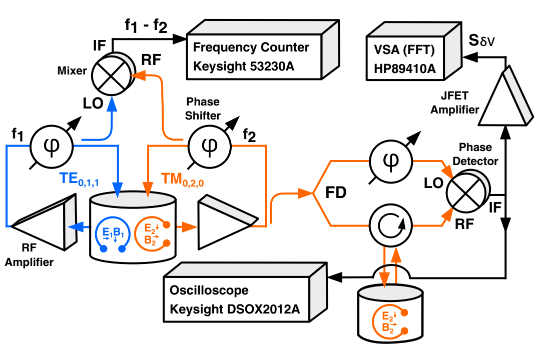

FIG. 1. UPLOAD-CMC schematic with frequency noise readout system. Loop oscillators support the microwave modes in the main resonator allowing axion conversion while a frequency counter records $|f_2 - f_1|$. The TM mode acts as the readout mode with constant f_2. The frequency noise is continuously scanned with a high-Q frequency discriminator (FD) based on a duplicate cavity, creating the frequency-phase dispersion required for voltage to frequency noise conversion of the mixer output.

$$\mathcal{H}_{\rm int} = \epsilon_0 c g_{a\gamma\gamma} a \mathbf{E}\cdot\mathbf{B}, \tag{1}$$

where $\mathbf{E}$ and $\mathbf{B}$ represent the electric and magnetic fields, a is the psuedoscalar axionlike field, c is the speed of light, ϵ_0 is the permittivity of free space, and $g_{a\gamma\gamma}$ is the axion-photon coupling strength [44]. The Hamiltonian can be expanded to account for the electric and magnetic field distributions of two photonic modes. The interaction may be rewritten in terms of creation and annihilation operators as

$$H_{\rm int} = i\pi\hbar g_{a\gamma\gamma} a\sqrt{f_1 f_2}[\xi_-(c_1 c_2^\dagger - c_1^\dagger c_2) + \xi_+(c_1^\dagger c_2^\dagger - c_1 c_2)], \tag{2}$$

where $\xi_\pm = -(\xi_{21} \pm \xi_{12})$ encodes the necessary mutual overlapping of the electric and magnetic field components of the two modes (see Ref. [20] as well as the Supplemental Material for more details) and f_1 and f_2 are the resonant frequencies of the photon modes. We find that the following regimes satisfy the Hamiltonian:

$$\begin{aligned} f_a &= f_2 + f_1 \text{ axion downconversion} \\ f_a &= |f_2 - f_1| \text{ axion upconversion} \end{aligned} \tag{3}$$

where $f_{1,2} \neq 0$. In essence, the axion field couples two microwave oscillators together when the axion frequency is at the sum or difference of the microwave frequencies, creating frequency or phase shifts in the microwave frequencies, arising from this trilinear coupling.

The phase shifts arise when we relax the frequency relations from Eq. (3) to

$$f_a = f_2 + f_1 \pm f \quad \text{or} \quad f_a = |f_2 - f_1| \pm f, \tag{4}$$

where $f \ll f_{1,2}$ represents a small offset. In this new relation, the axion amplitude becomes a slowly varying parameter in the equations of motion, inducing phase noise in the Fourier spectrum of both cavity modes, located at the offset frequency. A derivation of the transfer function from this slowly varying amplitude to resultant phase modulation can be found in Appendix B of Ref. [20]. Note, in the Supplemental Material we derive the resulting signal in terms of a fractional *frequency* modulation (related to phase noise), and use this approach throughout this work.

This induced modulation appears in the spectral density of fractional frequency fluctuations of the readout oscillator in the form

$$S_{Ay_2}(f)_\pm = g_{a\gamma\gamma}^2 k_{a\pm}^2 S_A(f), \qquad k_{a\pm}^2 = \pi^2 \frac{f_1 P_{c1}}{f_2 P_{c2}} \xi_\pm^2, \tag{5}$$

where P_{c1}/P_{c2} is the ratio of pump mode (subscript 1) and readout mode (subscript 2) circulating power in the resonator (see Fig. 1) and $\xi_\pm$ is the geometric overlap

TABLE I. Experimental microwave oscillator parameters.

	$TE_{0,1,1}$ (Mode 1 Fig. 1)	$TM_{0,2,0}$ (Mode 2 Fig. 1)
Q_L	6000	4200
β_{in}	0.9	0.95
P_{inc}	10 dBm	6 dBm
P_{c}	48 dBm	42 dBm
f_0	9.001 68–9.002 56 GHz	8.998 876 5 GHz
k_{a-}	5.5	
k_{a+}	$8.4 \times 10^{-4} - 1.1 \times 10^{-3}$	

factor, describing the efficiency of coupling between the two electromagnetic modes. Here $k_{a\pm}$ is the conversion ratio from axion theta angle, $\theta = g_{a\gamma\gamma} a$, to fractional frequency deviation, $y = (\delta f / f_0)$, with calculated values for this run shown in Table I. Here, the axion (or axionlike particle) field may be considered as a spectral density of narrow-band noise, centered at a frequency equivalent to the axion mass and broadened due to cold dark matter virilization to give a linewidth of $10^{-6} f_a$, and is denoted as $S_A(f)$ (kg/s/Hz) [45]. This must compete against the oscillator noise given by Leeson's model [46,47], which is typically of the form (see the Supplemental Material for more details and how to calculate the SNR)

$$S_{\phi_2}(f)_{\text{osc}} = S_{\phi_2}(f)_{\text{amp}} \left[1 + \left(\frac{\Delta f_{L_2}}{2f}\right)^2\right], \tag{6}$$

which can be converted to fractional frequency fluctuations via

$$S_{y_2}(f)_{\text{osc}} = \left(\frac{f}{f_2}\right)^2 S_{\phi_2}(f)_{\text{osc}}. \tag{7}$$

Here, $S_{\phi_2}(f)_{\text{amp}}$ is the phase noise of the amplifier in the feedback loop of the readout oscillator and Δf_{L_2} is the readout mode full bandwidth. For our free-running experiment, we find the SNR to be

$$\begin{aligned} \text{SNR}_- = g_{a\gamma\gamma} & \frac{2.7(\frac{10^6 t}{f_{a_-}})^{\frac{1}{4}} \sqrt{\rho_{\text{DM}} c^3}}{2\pi f_{a_-}} \\ & \times \sqrt{\frac{Q_{L2} P_{\text{amp}} (\beta_2 + 1)^2}{(F k_B T_0) \beta_2 P_2}} \sqrt{P_1 Q_{L1}} \\ & \times \sqrt{\frac{1}{(2 Q_{L2} \frac{f}{f_2})^2 + 1}}, \end{aligned} \tag{8}$$

explained in more detail in the Supplemental Material.

A cylindrical copper resonator was designed, in which two orthogonal modes could simultaneously oscillate. It was noted that a $TM_{0,2,0}$ mode offered a higher quality factor than a $TM_{0,1,0}$ mode without inducing significant mode crowding. A $TE_{0,1,1}$ mode was chosen for its wide frequency tuning range within the cavity and its optimal modal overlap with the chosen $TM_{0,2,0}$ mode. Specific parameters of the electromagnetic resonances are included in Table I and details of the overlap function are given in the Supplemental Material.

Two free-running loop oscillators were constructed from the TE and TM mode resonances, with the beat frequency under constant measurement via a RF mixer connected to a Keysight Frequency Counter (53230A). We chose to measure the frequency noise of the TM mode due to its relatively stationary frequency, which required minimal tuning of the frequency noise discrimination circuit, comprising a standard phase bridge, including a phase shifter, a double balanced mixer and a duplicate resonator included as the dispersive element. The reflected and phase-shifted signals were mixed in quadrature, such that the mixer output voltage was proportional to the frequency noise of the loop oscillator, including the frequency noise of the resonator where the axion signal is imprinted [48]. Essentially, the spectral density of fractional frequency fluctuations of the loop oscillator can be inferred from the measured spectral density of the voltage fluctuations output by the mixer, $S_v(f)$, by

$$S_{y_2}(f)_{\text{osc}} = \frac{S_{v_2}(f)}{f_2^2 k_f^2 G}, \tag{9}$$

where f_2 is the TM loop oscillator frequency and k_f and G, conversion efficiency and gain of the postamplifier. As an axion signal [Eq. (5)] must compete with the spread of this background to appear in the total frequency noise at the readout, frequency fluctuations in the oscillator and readout system are the limiting factor of this experiment.

Repeating measurements at slightly different detunings will cause a putative axion-induced signal to be correspondingly translated in the Fourier space of the measured noise spectrum. Therefore, the axion search involves combining several noise spectra and looking for evidence of a signal consistently satisfying Eq. (4) at a range of detunings. Figure 2 illustrates an example of a frequency noise spectrum filtered for the detection of a spurious RF signal. The minimum axion-photon coupling able to be statistically excluded by the data depends upon the distribution of this residual noise. The treatment of axion field strength follows Daw's convention [49] and the frequency noise is related to $g_{a\gamma\gamma}$ as per Eq. (5).

Experimental exclusion limits (Fig. 3) were produced via Monte Carlo simulations which were modeled upon the noise statistics of the experimental data. A minimum value for excludable axion-photon coupling was determined from these simulations by injecting axion signals (narrow-band frequency noise) of incremental $g_{a\gamma\gamma}$ [via Eq. (5)] upon simulated background spectra and identifying the value at

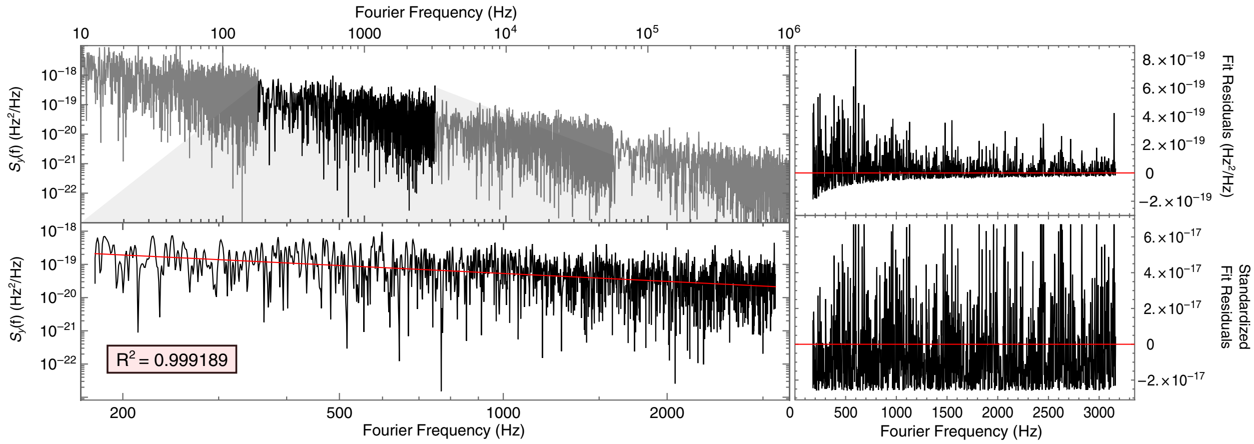

FIG. 2. Top left: Filtered spectral density of fractional frequency noise at Fourier frequencies about the normal mode frequency, f_{TM}, for $f_{\mathrm{TM}} = 8.9989$ GHz and $f_{\mathrm{TE}} = 9.00241$ GHz. Bottom left: The second decade of data, with inverse power law fit. Decades were analyzed independently. Top right: Residuals from the spectral density of fractional frequency noise fit, examinable as axion-induced excesses. Bottom right: Standardized residuals (henceforth referred to as "search spectrum amplitudes"), ready to be interrogated with the axion-search procedure.

which the threshold was correctly triggered in 95% of cases. The injected signal assumed a thermalized dark matter halo with a Maxwell-Boltzmann velocity distribution near the Earth with $v_c = 225\ \mathrm{km\,s^{-1}}$ [45]. Further effects on the axion line shape were built into the simulation based on the drift of the microwave frequencies, which was ~5 Hz per measurement, varying per measurement.

To improve the SNR, a multibin search (similar to Daw's method [49]) was used, where n translated arrays of n-bin averages were examined for axion signals, mitigating the effect of adjacent bin power loss. After binning, data points above our candidate threshold were isolated for examination, as, according to our noise model, the probability of the background noise breaching this level was 0.05% (detailed in the Supplemental Material). A candidate breaching this threshold must be eliminated by examining data taken at an offset microwave detuning.

Data was taken with the TE mode tuned 2.8, 3.1, 3.3, 3.5, and 3.7 MHz above the TM mode frequency, accessing axion frequencies in the MHz range by upconversion. An approximate tuning interval of 300 kHz was chosen to enable tracking of candidate signals between measurements. The experimental data have excluded axions in the probed mass range with an axion-photon coupling exceeding the limits illustrated in Fig. 3.

The next iteration of UPLOAD-CMC will benefit from measurement automation and statistically optimal overlapped binning, width scaling with axion frequency [49]. Measurements will begin at the lowest feasible beat frequency supported by the current experiment (about 300 kHz, limited by parasitic coupling between the modes) and progress upwards in frequency space. Integration time will be increased to days per MHz and the noise filter will be recalibrated every five tuning steps. Figure 3 illustrates the sensitivities expected to be achievable using frequency-stabilized (as opposed to free-running) loop oscillators at room temperature, as well as a Nb resonator operating at the noise floor of the frequency discriminator at cryogenic temperatures near 4 K, assuming loop-sustaining amplifiers of an effective noise temperature of 8 K [60], at 30 days per MHz. The projected exclusion limits in Fig. 3 were produced by setting the theoretical SNR of various setups to unity and solving for $g_{a\gamma\gamma}$ (detailed in the Supplemental Material).

As the oscillator phase or frequency noise is directly related to axion sensitivity, increasing phase stability is our most direct avenue of improvement, and is highly possible with modern equipment and techniques, which is discussed comprehensively in the Supplemental Material. For example, the single sideband phase noise of the oscillator in this work was measured to be approximately -60 dBc/Hz at 1 kHz offset (conforming with Leeson's model for this oscillator with an amplifier of $F = 2.6$ at $P_{\mathrm{amp}} = -33$ dBm and $T = 300$ K), which is far noisier than the state-of-the-art oscillators using specialized frequency locking and high-Q cavities. For example, a phase noise of -160 dBc/Hz at 1 kHz Fourier frequency and at room temperature has been measured [61]; a 10 order-of-magnitude improvement over our experiment. Recently, a path forward to realizing a phase noise of -185 dBc/Hz at offsets above 300 Hz has been proposed [60] meaning QCD axion sensitivity could be feasible in the future. QCD axion sensitivity may also be achievable by UPLOAD-CM-III-Cryo at extremely low axion masses (< 1.8 kHz, i.e., 7.7×10^{-12} eV) if the geometry is tuned to sustain orthogonal modes with equivalent resonant frequencies such that $f_2 \sim f_1$, so that $f_a = f$. We refer to this as the degenerate configuration of the experiment.

Our results demonstrate the feasibility of exploiting frequency metrology to develop highly sensitive axion

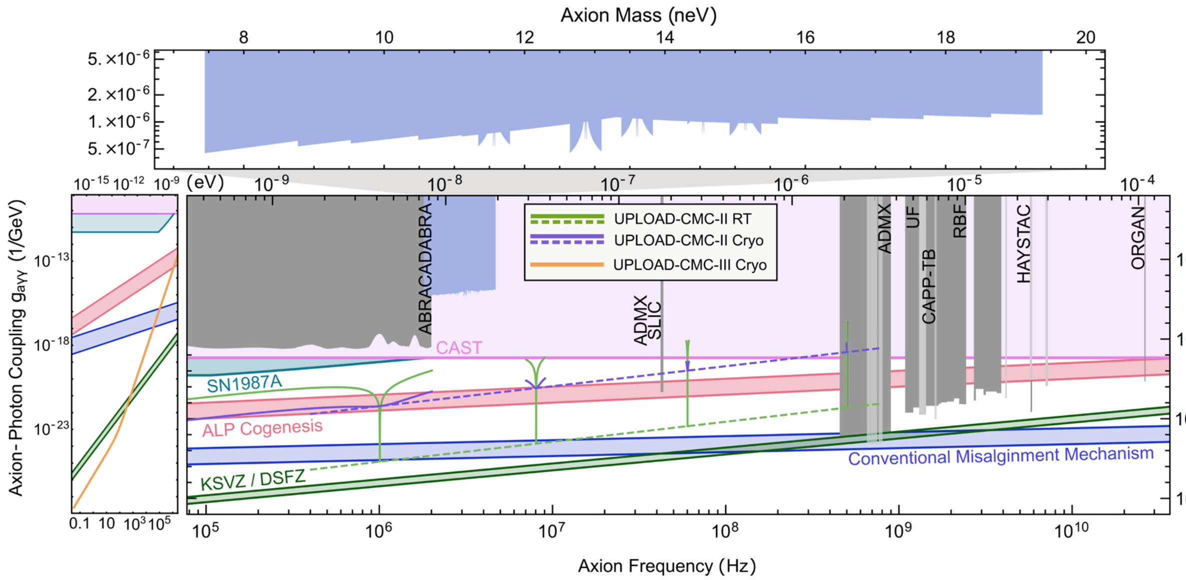

FIG. 3. The 95% confidence exclusion zone for $g_{a\gamma\gamma}$ (in natural units) for the measured mass range (top), with CAST's helioscope limits and popular QCD axion models in green (KSVZ and DSFZ) [1,50], blue (conventional ALP misalignment), and red (ALP cogenesis) [51,52]. Projected upconversion limits are dashed, illustrating best limits throughout the range in 1 Hz tuning steps (30 days per Hz): UPLOAD-CMC-II-RT, a copper resonator with frequency stabilized (FS) loops at room temperature (RT); and UPLOAD-CMC-II-Cryo, cryogenic Nb with FS loops. These dashed limits represent sensitivity at a uniform Fourier offset, and so it would be temporally infeasible to scan the entire range at the represented level. Since a real stationary measurement has sensitivity varying within the Fourier range, we also present examples of 30 day measurements covering 1 MHz in Fourier space, in bold. Projections are based on readily constructible setups with available equipment and standard techniques. With a similar setup as for UPLOAD-CMC-II-Cryo, in UPLOAD-CMC-III-Cryo we expect to reach QCD axion limits at very low upconversion energies (< 1.8 kHz, i.e., 7.7×10^{-12} eV) by tuning the orthogonal modes to coincide in resonant frequency (to reach the sensitivity illustrated in the left subplot, 1.3 years of data acquisition is necessary). Excluded axion space by ADMX [13–15,53], ORGAN [16], ABRACADABRA [54], ADMX-SLIC [55], HAYSTAC [56], UF [57], CAPP-8TB [58], and RBF [59] is also represented.

dark matter detectors, with the potential to search wide regions of unexplored axion mass. Proof of principle was achieved with an integration time on the order of just hours, allowing a coupling strength of 5×10^{-7} 1/ GeV to be excluded between 7.44–19.38 neV. Appraising spectacular modern advances in low phase noise oscillators, a roadmap has been laid to reach axion model limits with future experiments at room temperature and at cryogenic temperatures using this novel axion-search technique.

This work was funded by the ARC Centre of Excellence for Engineered Quantum Systems, CE170100009, and the ARC Centre of Excellence for Dark Matter Particle Physics, CE200100008, as well as ARC Grant No. DP190100071.

*catriona.thomson@research.uwa.edu.au
†michael.tobar@uwa.edu.au

[1] P. W. Graham, I. G. Irastorza, S. K. Lamoreaux, A. Lindner, and K. A. van Bibber, Experimental searches for the axion and axion-like particles, Annu. Rev. Nucl. Part. Sci. **65**, 485 (2015).

[2] R. D. Peccei and H. R. Quinn, *CP* Conservation in the Presence of Instantons, Phys. Rev. Lett. **38**, 1440 (1977).

[3] G. Bertone, *Particle Dark Matter: Observations, Models and Searches* (Cambridge University Press, Cambridge, England, 2010).

[4] F. Wilczek, Problem of Strong *P* and *T* Invariance in the Presence of Instantons, Phys. Rev. Lett. **40**, 279 (1978).

[5] M. S. Turner, Windows on the axion, Phys. Rep. **197**, 67 (1990).

[6] R. D. Peccei, The Strong *CP* problem and axions, Lect. Notes Phys. **741**, 3 (2008).

[7] G. Ballesteros, J. Redondo, A. Ringwald, and C. Tamarit, Unifying Inflation with the Axion, Dark Matter, Baryogenesis, and the Seesaw Mechanism, Phys. Rev. Lett. **118**, 071802 (2017).

[8] J. Jaeckel, E. Massó, J. Redondo, A. Ringwald, and F. Takahashi, Need for purely laboratory-based axionlike particle searches, Phys. Rev. D **75**, 013004 (2007).

[9] P. Sikivie, Experimental Tests of the "Invisible" Axion, Phys. Rev. Lett. **52**, 695(E) (1984).

[10] Y. Kim, D. Kim, J. Jeong, J. Kim, Y. Chang Shin, and Y. K. Semertzidis, Effective approximation of electromagnetism for axion haloscope searches, Phys. Dark Universe **26**, 100362 (2019).

[11] M. E. Tobar, B. T. McAllister, and M. Goryachev, Modified axion electrodynamics as impressed electromagnetic sources through oscillating background polarization and magnetization, Phys. Dark Universe **26**, 100339 (2019).

[12] M. E. Tobar, B. T. McAllister, and M. Goryachev, Broadband electrical action sensing techniques with conducting wires for low-mass dark matter axion detection, Phys. Dark Universe **30**, 100624 (2020).

[13] N. Du, N. Force, R. Khatiwada, E. Lentz, R. Ottens *et al.*, Search for Invisible Axion Dark Matter with the Axion Dark Matter Experiment, Phys. Rev. Lett. **120**, 151301 (2018).

[14] C. Boutan, M. Jones, B. H. LaRoque, N. S. Oblath, R. Cervantes *et al.*, Piezoelectrically Tuned Multimode Cavity Search for Axion Dark Matter, Phys. Rev. Lett. **121**, 261302 (2018).

[15] T. Braine *et al.*, Extended Search for the Invisible Axion with the Axion Dark Matter Experiment, Phys. Rev. Lett. **124**, 101303 (2020).

[16] B. T. McAllister, G. Flower, E. N. Ivanov, M. Goryachev, J. Bourhill, and M. E. Tobar, The organ experiment: An axion haloscope above 15 ghz, Phys. Dark Universe **18**, 67 (2017).

[17] A. Droster and K. van Bibber, HAYSTAC status, results, and plans, in *13th Conference on the Intersections of Particle and Nuclear Physics (CIPANP), 2018*, 2019.

[18] W. Chung, CULTASK, the coldest axion experiment at CAPP/IBS in Korea, in *Proceedings of the Corfu Summer Institute 2015* (2016), Vol. 263, p. 047.

[19] P. Sikivie, Superconducting radio frequency cavities as axion dark matter detectors, arXiv:1009.0762.

[20] M. Goryachev, B. T. McAllister, and M. E. Tobar, Axion detection with precision frequency metrology, Phys. Dark Universe **26**, 100345 (2019).

[21] R. Lasenby, Microwave cavity searches for low-frequency axion dark matter, arXiv:1912.11056.

[22] R. Lasenby, Parametrics of electromagnetic searches for axion dark matter, arXiv:1912.11467.

[23] See Supplemental Material at http://link.aps.org/supplemental/10.1103/PhysRevLett.126.081803 for further technical experimental details and methods not detailed in the main body, which includes Refs. [24–37].

[24] S. Buchman, J. P. Turneaure, and J. Lipa, Prospects for an improved superconducting cavity stabilized oscillator clock, in *30th Rencontres de Moriond: Euroconferences: Dark Matter in Cosmology, Clocks and Tests of Fundamental Laws* (Ed. Frontieres, Gif-Sur-Yvette, 1995).

[25] M. Checchin and M. Martinello, Analytic solution of the electromagnetic eigenvalues problem in a cylindrical resonator, arXiv:1610.02083.

[26] D. Halford, J. H. Shoaf, and A. S. Risley, Spectral density analysis: Frequency domain specification and measurement of signal stability, in *27th Annual Symposium on Frequency Control* (IEEE, New York, 1973), pp. 421–431.

[27] E. N. Ivanov, M. E. Tobar, and R. A. Woode, Microwave interferometry: Application to precision measurements and noise reduction techniques, IEEE Trans. Ultrason. Ferroelectric Freq. Control **45**, 1526 (1998).

[28] E. N. Ivanov, J. G. Hartnett, and M. E. Tobar, Cryogenic microwave amplifiers for precision measurements, IEEE Trans. Ultrason. Ferroelectric Freq. Control **47**, 1273 (2000).

[29] E. N. Ivanov and M. E. Tobar, Microwave phase detection at the level 10^{-11}, Rev. Sci. Instrum. **80**, 044701 (2009).

[30] E. N. Ivanov, S. R. Parker, R. Bara-Maillet, and M. E. Tobar, Noise properties of cryogenic microwave amplifiers and relevance to oscillator frequency stabilization, IEEE Trans. Ultrason. Ferroelectric Freq. Control **61**, 575 (2014).

[31] M. Martinello, M. Checchin, A. Romanenko, A. Grassellino, S. Aderhold, S. K. Chandrasekeran, O. Melnychuk, S. Posen, and D. A. Sergatskov, Field-Enhanced Superconductivity in High-Frequency Niobium Accelerating Cavities, Phys. Rev. Lett. **121**, 224801 (2018).

[32] D. B. Sullivan, D. W. Allan, D. A. Howe, and F. L. Walls, Characterization of clocks and oscillators, NIST Technical Note (1337), 1990.

[33] J. Rutman and F. L. Walls, Characterization of frequency stability in precision frequency sources, Proc. IEEE **79**, 952 (1991).

[34] S. R. Stein and J. P. Turneaure, Superconducting-cavity-stabilised oscillator of high stability, Electron. Lett. **8**, 321 (1972).

[35] S. R. Stein and J. P. Turneaure, Superconducting-cavity stabilized oscillators with improved frequency stability, Proc. IEEE **63**, 1249 (1975).

[36] M. E. Tobar, A. J. Giles, S. Edwards, and J. H. Searls, High-q thermoelectric-stabilized sapphire microwave resonators for low-noise applications, IEEE Trans. Ultrason. Ferroelectric Freq. Control **41**, 391 (1994).

[37] M. Edmund Tobar, P. Wolf, A. Fowler, and J. Gideon Hartnett, New methods of testing Lorentz violation in electrodynamics, Phys. Rev. D **71**, 025004 (2005).

[38] J. P. Turneaure, C. M. Will, B. F. Farrell, E. M. Mattison, and R. F. C. Vessot, Test of the principle of equivalence by a null gravitational red-shift experiment, Phys. Rev. D **27**, 1705 (1983).

[39] M. Edmund Tobar, P. Wolf, S. Bize, G. Santarelli, and V. Flambaum, Testing local Lorentz and position invariance and variation of fundamental constants by searching the derivative of the comparison frequency between a cryogenic sapphire oscillator and hydrogen maser, Phys. Rev. D **81**, 022003 (2010).

[40] M. E. Tobar, P. L. Stanwix, J. J. McFerran, J. Guena, M. Abgrall, S. Bize, A. Clairon, Ph. Laurent, P. Rosenbusch, D. Rovera, and G. Santarelli, Testing local position and fundamental constant invariance due to periodic gravitational and boost using long-term comparison of the SYRTE atomic fountains and H-masers, Phys. Rev. D **87**, 122004 (2013).

[41] M. Nagel, S. R. Parker, E. V. Kovalchuk, P. L. Stanwix, J. G. Hartnett, E. N. Ivanov, A. Peters, and M. E. Tobar, Direct terrestrial test of lorentz symmetry in electrodynamics to 10^{-18}, Nat. Commun. **6**, 8174 (2015).

[42] A. Lo, P. Haslinger, E. Mizrachi, L. Anderegg, H. Müller, M. Hohensee, M. Goryachev, and M. E. Tobar, Acoustic Tests of Lorentz Symmetry Using Quartz Oscillators, Phys. Rev. X **6**, 011018 (2016).

[43] M. Goryachev, Z. Kuang, E. N. Ivanov, P. Haslinger, H. Muller, and M. E. Tobar, Next generation of phonon tests of Lorentz invariance using quartz BAW resonators, IEEE Trans. Ultrason. Ferroelectric Freq. Control **65**, 991 (2018).

[44] A. Ringwald, Exploring the role of axions and other wisps in the dark universe, Phys. Dark Universe **1**, 116 (2012).

[45] E. W. Lentz, T. R. Quinn, L. J. Rosenberg, and M. J. Tremmel, A new signal model for axion cavity searches from N-body simulations, Astrophys. J. **845**, 121 (2017).

[46] D. B. Lesson, A simple model of feedback oscillator noise spectrum, Proc. IEEE **54**, 329 (1966).

[47] A. L. Lance, W. D. Seal, and F. Labaar, Phase noise and am noise measurements in the frequency domain, Infrared Millimeter Waves **11**, 239 (1984), https://tf.nist.gov/general/tn1337/Tn190.pdf.

[48] A. S. Risley J. H. Shoaf and D. Halford, Nbs tech. note 632, Technical report, 1973.

[49] E. John Daw, A search for halo axions, Ph.D. thesis, Massachusetts Institute of Technology, 1998.

[50] V. Anastassopoulos *et al.*, New cast limit on the axion—photon interaction, Nat. Phys. **13**, 584 (2017).

[51] R. T. Co, L. J. Hall, and K. Harigaya, Predictions for axion couplings from ALP cogenesis, arXiv:2006.04809.

[52] R. T. Co, L. J. Hall, and K. Harigaya, Axion Kinetic Misalignment Mechanism, Phys. Rev. Lett. **124**, 251802 (2020).

[53] C. Bartram *et al.* (ADMX Collaboration), Axion dark matter experiment: Run 1b analysis details, arXiv:2010.06183.

[54] R. Henning *et al.*, First Results from ABRACADABRA-10 cm: A Search for Sub-μev Axion Dark Matter, Phys. Rev. Lett. **122**, 121802 (2019).

[55] N. Crisosto, P. Sikivie, N. S. Sullivan, D. B. Tanner, J. Yang, and G. Rybka, ADMX SLIC: Results from a Superconducting LC Circuit Investigating Cold Axions, Phys. Rev. Lett. **124**, 241101 (2020).

[56] B. M. Brubaker, L. Zhong, Y. V. Gurevich, S. B. Cahn, S. K. Lamoreaux *et al.*, First Results from a Microwave Cavity Axion Search at 24 μeV, Phys. Rev. Lett. **118**, 061302 (2017).

[57] C. Hagmann, P. Sikivie, N. S. Sullivan, and D. B. Tanner, Results from a search for cosmic axions, Phys. Rev. D **42**, 1297 (1990).

[58] S. Lee, S. Ahn, J. Choi, B. R. Ko, and Y. K. Semertzidis, Axion Dark Matter Search around 6.7μeV, Phys. Rev. Lett. **124**, 101802 (2020).

[59] W. U. Wuensch, S. De Panfilis-Wuensch, Y. K. Semertzidis, J. T. Rogers, A. C. Melissinos, H. J. Halama, B. E. Moskowitz, A. G. Prodell, W. B. Fowler, and F. A. Nezrick, Results of a laboratory search for cosmic axions and other weakly coupled light particles, Phys. Rev. D **40**, 3153 (1989).

[60] E. N. Ivanov and M. E. Tobar, Generation of spectrally pure microwave signals, arXiv:2003.09117.

[61] E. N. Ivanov and M. E. Tobar, Low phase-noise microwave oscillators with interferometric signal processing, IEEE Trans. Microwave Theory Tech. **54**, 3284 (2006).